



# Freeze–thaw effects on erosion process in loess slope under simulated rainfall

SU Yuanyi<sup>1,2</sup>, LI Peng<sup>1,2\*</sup>, REN Zongping<sup>1,2</sup>, XIAO Lie<sup>1,2</sup>, ZHANG Hui<sup>3</sup>

<sup>1</sup> State Key Laboratory of Eco-hydraulics in Northwest Arid Region of China, Xi'an University of Technology, Xi'an 710048, China;

<sup>2</sup> Key Laboratory of National Forestry Administration on Ecological Hydrology and Disaster Prevention in Arid Regions, Xi'an 710048, China;

<sup>3</sup> China JIKAN Research Institute of Engineering Investigations and Design Co. Ltd., Xi'an 710048, China

**Abstract:** Seasonal freeze–thaw processes have led to severe soil erosion in the middle and high latitudes. The area affected by freeze–thaw erosion in China exceeds 13% of the national territory. So understanding the effect of freeze–thaw on erosion process is of great significance for soil and water conservation as well as for ecological engineering. In this study, we designed simulated rainfall experiments to investigate soil erosion processes under two soil conditions, unfrozen slope (UFS) and frozen slope (FS), and three rainfall intensities of 0.6, 0.9 and 1.2 mm/min. The results showed that the initial runoff time of FS occurred much earlier than that of the UFS. Under the same rainfall intensity, the runoff of FS is 1.17–1.26 times that of UFS; and the sediment yield of FS is 6.48–10.49 times that of UFS. With increasing rainfall time, rills were produced on the slope. After the appearance of the rills, the sediment yield on the FS accounts for 74%–86% of the total sediment yield. Rill erosion was the main reason for the increase in soil erosion rate on FS, and the reduction in water percolation resulting from frozen layers was one of the important factors leading to the advancement of rills on slope. A linear relationship existed between the cumulative runoff and the sediment yield of UFS and FS ( $R^2 > 0.97$ ,  $P < 0.01$ ). The average mean weight diameter (MWD) on the slope erosion particles was as follows: UFS0.9 (73.84  $\mu\text{m}$ ) > FS0.6 (72.30  $\mu\text{m}$ ) > UFS1.2 (72.23  $\mu\text{m}$ ) > substrate (71.23  $\mu\text{m}$ ) > FS1.2 (71.06  $\mu\text{m}$ ) > FS0.9 (70.72  $\mu\text{m}$ ). During the early stage of the rainfall, the MWD of the FS was relatively large. However, during the middle to late rainfall, the particle composition gradually approached that of the soil substrate. Under different rainfall intensities, the mean soil erodibility (MK) of the FS was 7.22 times that of the UFS. The ratio of the mean regression coefficient  $C_2$  ( $MC_2$ ) between FS and UFS was roughly correspondent with MK. Therefore, the parameter  $C_2$  can be used to evaluate soil erodibility after the appearance of the rills. This article explored the influence mechanism of freeze–thaw effects on loess soil erosion and provided a theoretical basis for further studies on soil erosion in the loess hilly regions.

**Keywords:** unfrozen slope (UFS); frozen slope (FS); simulated rainfall; soil size selectivity; soil erodibility; loess hilly region

**Citation:** SU Yuanyi, LI Peng, REN Zongping, XIAO Lie, ZHANG Hui. 2020. Freeze–thaw effects on erosion process in loess slope under simulated rainfall. *Journal of Arid Land*, 12(6): 937–949. <https://doi.org/10.1007/s40333-020-0106-6>

## 1 Introduction

Seasonal freeze–thaw cycles occur mainly in middle latitudes and are generally characterized by winter frozen and summer ablation (Bochove, 2000; Sahin and Anapali, 2007; Dagesse et al., 2010;

\*Corresponding author: LI Peng (E-mail: lipeng74@163.com)

Received 2020-03-21; revised 2020-10-08; accepted 2020-10-15

© Xinjiang Institute of Ecology and Geography, Chinese Academy of Sciences, Science Press and Springer-Verlag GmbH Germany, part of Springer Nature 2020

Ren et al., 2018; Wang et al., 2018; Su et al., 2020). According to the Second National Soil Erosion Remote Sensing Survey, the area of freeze-thaw erosion in China is more than  $126.98 \times 10^4 \text{ km}^2$ , accounting for 13.4% of the total national land area (Wang et al., 2020). The middle reaches of the Yellow River (China) are subject to these cycles due to soil temperatures below  $0^\circ\text{C}$  and down to  $-15^\circ\text{C}$  between the end of October and the end of March next year. The soil temperature was below  $0^\circ\text{C}$  for a total of 110 d (Li and Fan, 2014; Cheng et al., 2018). The climatic conditions in the region meet the requirements for freeze-thaw erosion. During the freeze-thaw cycle period, the soil thaws in the morning and freezes again at night with decreasing temperatures. Soil combines with melting water, resulting in upper slope soil detachment and downstream sediment transport in rivers. Previous studies showed that the sediment yield of freeze-thaw combined erosion in the loess hilly-gully region can reach at least 30% of channel erosion (Wang et al., 2004). The freeze-thaw of soil have both direct and indirect effects on the physical and chemical properties of soil (Ferrick and Gatto, 2005; Li et al., 2012). Studies also showed that freeze-thaw cycles can effectively change the soil structure (Pawluk et al., 1988; Henry et al., 2007), thereby reducing the soil shear strength and increasing soil erodibility (Wang et al., 2015). Through laboratory tests, Edwards and Burney (1989) found that the amount of sediment yield after a freeze-thaw cycle increased by about 25%. When the soil is in a frozen state, the volume expansion of the soil water led to destroy the bonds between soil particles, thereby changing aggregate size distribution (Cruse et al., 2001). The freeze-thaw causes the soil particle size to decrease, which has a major impact on water erosion (Layton et al., 1993; Oztas and Fayetorbay, 2003). In the partial freeze-thaw erosion zone, the incompletely thawed layer is one of the important factors affecting the soil erosion during the spring thawing period (Wischmeier et al., 1971). The frozen soil hinders water infiltration, which lead to generate greater runoff. Therefore, a large amount of sediment was separated and transported under runoff. Kirkby (1980) stated that half of the annual soil erosion in the temperate zone occurs due to the thawing of frozen soils. When the frozen soil thaws, its shear strength decreases, and its erodibility increased, thus making the soil in the thawing period more susceptible to loss (Ting et al., 1983). Sharratt et al. (2000) found that the impervious frozen layer in the soil during the thawing period is the main factor leading to the increase of soil erosion. Previous studies mainly focused on the changes of soil erodibility before and after the freeze-thaw cycle but a few on the erodibility of partially frozen soil.

The size distribution of eroded sediment during the erosion process can well reflect the changing processes occurring during erosion (Bullock et al., 1988; Wang et al., 2017). Asadi et al. (2007) and Wang et al. (2014) found that the content of clay and silt in the eroded sediment is higher during the beginning of erosion. As the erosion time prolongs, the sediment size gradually becomes larger and finally stabilizes. The size distribution of eroded soil depends on many factors such as the soil texture, rainfall characteristics, runoff type, freeze-thaw and topographical characteristics (Issa et al., 2006; Shi et al., 2012; Koiter et al., 2013). These factors affect soil aggregation. Under the combined action of rainfall and freeze-thaw cycles, the slope erosion and sediment particle separation rules may be very different from those of the single hydraulic erosion case (Wischmeier and Smith, 1965). However, the erosion and sediment separation processes under this combined erosion have not been fully understood yet (Wang et al., 2013).

Due to the differences in surface conditions and climate change, large differences exist with regards to the characteristics of soil erosion during the thawing period among various local areas in the middle reaches of the Yellow River. These differences may affect the soil erosion in turn impacting soil dislodgement and transport. In this study, the analyses of soil erosion processes under different treatments were conducted through indoor simulated rainfall experiments, and focused on the influence of thawing of frozen soil on soil erosion and sediment size distribution, so as to provide a baseline for further understanding of the soil water erosion mechanism of thawing slopes.

## 2 Materials and methods

### 2.1 Materials and devices

The soil was taken from the abandoned farmland of the Wangmaogou watershed ( $37^\circ34'13''$ –

37°36′03″N, 110°20′46″–110°22′46″E) located in the Loess Plateau of China. This region is within the temperate semi-arid continental monsoon climate zone, with an annual mean temperature of 10°C, a maximum of 39°C in July and a minimum of –27°C in January (Zhao et al., 2017; Chang et al., 2019a, b). Therefore, during winter and early spring, soil goes through several freeze–thaw cycles. The watershed is a two-branched depression on the left bank of the Wuding River, with an area of 5.97 km<sup>2</sup>. The mean annual precipitation is 475 mm in the basin (Xiao et al., 2019a, b). The land use types in the basin are mainly grassland, sloping farmland, terraced land and woodland (Shi et al., 2019, 2020). Soil particle size was obtained using a Mastersizer 2000 sediment particle size analyser (Malvern Instruments, UK). This analysis revealed that the clay, silt and sand accounted for 0.20%, 72.01% and 27.79%, respectively. The soil was identified as silt loam according to the soil classification standard of the USDA (United States Department of Agriculture). The dry bulk density of the soil is about 1.3 g/cm<sup>3</sup>, organic matter content is 2.0 g/kg (Zhang et al., 2019) and the saturated water content is 46.41%.

The test device consists of three parts: the frozen soil system, the test soil trough and the rainfall system. The frozen soil system (4.5 m (length)×2.5 m (width)×2.5 m (height)) adopts the freeze–thaw test system of Xi'an University of Technology. The temperature variation range is –40°C–30°C (±1°C), which can meet the test requirements. The soil tank is a wooden impervious structure, with the corners and the periphery fixed by angle iron anchors, and the soil tank mounted on a trolley so it can be moved. The size of the box holding the soil is 2.00 m long, 0.75 m wide and 0.35 m deep. A flume collects runoff and sediment at the lower end of the soil box (Fig. 1a). A rainfall simulator is used with different nozzle types to vary rainfall intensity. The nozzle is mounted 5.2 m above the soil surface to guarantee drops reached terminal velocity, and the rainfall intensity varies from 0.5 to 2.0 mm/min (Fig. 1b).

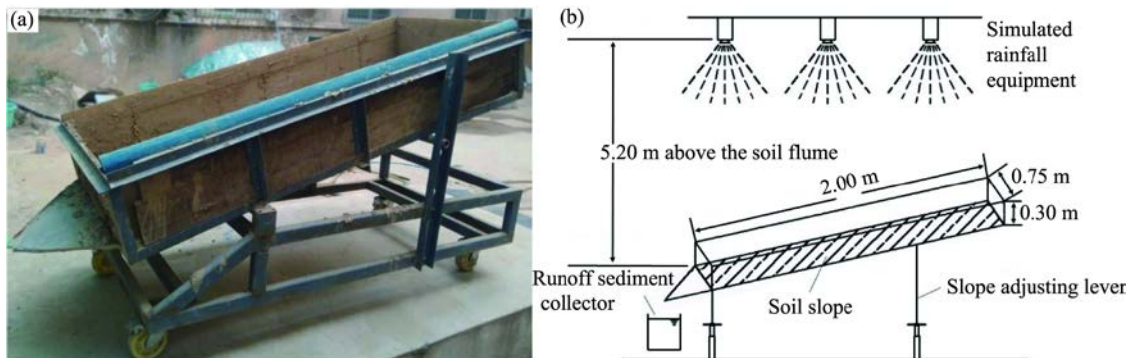


**Fig. 1** Experimental device diagrams of test equipment real diagram (a) and schematic diagram of the simulated rainfall system (b)

## 2.2 Experimental design

The simulated rainfall experiments were implemented at the State Key Laboratory of Eco-hydraulics in Northwest Arid Region of China (Xi'an University of Technology) in Xi'an in October 2016. The experiment included two kinds of slopes (unfrozen slope (UFS) and frozen slope (FS)) and three rainfall intensities (0.6, 0.9 and 1.2 mm/min). Each experiment was replicated three times and the experimental results are the average of three replicates. To ensure that the initial conditions of the rainfall simulation experiments were consistent, the design grade was set to 15°. The rainfall temperature during the test were maintained at 15°C. Before the test, the soil samples collected in the field were passed through a 5 mm sieve, and the roots, stones and other debris were removed. The soil samples were then moistened so that the water content reached about 15%. Before filling the box with soil, a layer of gauze was laid on the bottom of the soil tank and a 5-cm thick layer of sand was placed on top of the gauze. According to the designed dry bulk density of the soil samples (1.30 g/cm<sup>3</sup>), the box was filled with 5-cm thick layers of soil at a time, following which the topsoil was slightly roughened before the next layer was laid to ensure that the two layers of soil samples were closely combined. The depth of soil was 20 cm. In order to avoid the influence of the wall on

the erosion process, the slope is designed to be high in the middle and low on both sides. Soil boxes of the unfrozen slope were kept in the laboratory under 5°C–8°C room temperature. Some of the soil boxes were put inside the freezer, and the soil was frozen for at least 24 h under –18°C to –22°C, making sure the soil in the box was completely frozen. Soil boxes of the frozen slope were used to carry out the experiment immediately. In order to prevent soil moisture from evaporating, all soil boxes were covered with plastic film, which was removed just before the test.

The rainfall intensity was determined before test. The uniformity was measured by six rainfall gauges. And the uniformity was measured three times before test and take the average value. When the uniformity of the rainfall was greater than 85% and the difference between the measured rainfall intensity and the target rainfall intensity was less than 5%, the subsequent formal rainfall test could be performed. The runoff duration was set to last for 60 min. Runoff and sediment in the storage bucket were collected every three minutes and the runoff volume was measured. Sediment was separated after settling the muddy water, before being dried at 105°C for 24 h and subsequently weighed. The sediments were sieved through a 2 mm mesh for determining particle size composition using the Mastersizer 2000. Pretest results showed that no runoff occurs on the slope under 0.6 mm/min rainfall intensity. Therefore, in the later tests, the rainfall erosion process of the slope under the rainfall intensity of 0.6 mm/min was not analyzed.

### 2.3 Measurements and data analyses

The particle sorting characterizing the erosion process is expressed by the mean weight diameter (MWD; Bissonnais, 1996). Sediment size distribution was calculated as follows:

$$\text{MWD} = \frac{\sum_{i=1}^7 x_i w_i}{100}, \quad (1)$$

where  $x_i$  is the mean diameter of the  $i$  size class (mm);  $w_i$  is the percentage of particles of the  $i$  size class (%); and  $i$  is divided into seven grades (<0.005, 0.005–0.100, 0.100–0.200, 0.200–0.500, 0.500–1.000, 1.000–2.000 and >2.000 mm).

The data used to estimate the soil erodibility in this study were obtained by an indoor simulated rainfall test. The formula for calculating the soil erodibility factor  $K$  in the Universal Soil Loss Equation (USLE; Weindorf, 2006) is:

$$K = A / (R \times L \times S \times C \times P), \quad (2)$$

where  $K$  is the soil erodibility (kg·h/(MJ·mm));  $A$  is the amount of soil loss (kg/m<sup>2</sup>);  $R$  is the rainfall erosivity factor (MJ·mm/(m<sup>2</sup>·h));  $L$  is the slope length factor;  $S$  is the slope factor;  $C$  is the crop management factor; and  $P$  is the management practice factor. The factors  $C$  and  $P$  are set to 1 under the conditions of this test.

A one way ANOVA (analysis of variance) and Duncan's multiple range test were used to ascertain whether the differences between the indicators and ratios were significant ( $P=0.05$ ). All statistical analyses were conducted using SPSS 21.0 (IBM, USA). Figures were generated in Origin 8.5 (OriginLab, USA). The Photoshop (Adobe Systems Incorporated, USA) was applied to design the simulated rainfall system.

## 3 Results

### 3.1 Characteristics of runoff and sediment yield under different treatments

#### 3.1.1 Characteristics of runoff and sediment yield

In both the FS and UFS, rills appeared during the rainfall process, but the timing of rill occurrence under similar hydraulic conditions was different for the two slopes (Table 1), with results also seemingly different (Fig. 2). According to relevant theories and experimental phenomena, the amount of erosion will increase sharply after rill occurred (Shen et al., 2016). These experiments took the time of rills occurrence as the limit, which divided the erosion process into two stages: before the appearance of the rills (I-stage) and after the appearance of the rills (II-stage). The sulcus formed on the UFS was shorter and shallower (Fig. 2a), while the gully of the FS had a higher level.

**Table 1** Slope runoff, sediment yield and its main moments

Treatment	Initial runoff time (min)	Time of rill appearance (min)	Average value		
			Runoff rate (mm/min)	Sediment yield rate during the I -stage (g/min)	Sediment yield rate during the II -stage (g/min)
UFS0.9	24.2	42	532.30	13.97	62.67
UFS1.2	9.0	33	878.62	19.67	121.46
FS0.6	10.1	27	233.45 <sup>a</sup>	38.08 <sup>a</sup>	125.72 <sup>a</sup>
FS0.9	5.5	21	620.28 <sup>b</sup>	134.24 <sup>b</sup>	382.24 <sup>b</sup>
FS1.2	2.6	12	1104.61 <sup>c</sup>	139.65 <sup>b</sup>	523.00 <sup>c</sup>

Note: UFS, unfrozen slope; FS, frozen slope; 0.6, 0.9 and 1.2 after UFS and FS are different rainfall intensities (mm/min). I -stage, before the appearance of the rills; II -stage, after the appearance of the rills. For FS, the different lowercase letters represent significant differences between different rainfall intensities.

**Fig. 2** Topography of the unfrozen slope (UFS; a) and frozen slope (FS; b) under 1.2 mm/min rainfall intensity

of development and longer rills (Fig. 2b). The development speed and extent of rills directly affect the intensity of slope erosion. For the same rainfall intensity, the runoff time of the FS was much smaller than that of the UFS. The initial runoff time of FS under the rainfall intensities of 0.9 and 1.2 mm/min was 18.7 and 6.4 min earlier than those of the UFS, respectively. As the rainfall intensity increased, the runoff rate of the slope increased significantly. When the rainfall intensity was increased from 0.9 to 1.2 mm/min, the runoff rates of the FS and the UFS increased 78.08% and 65.06%, respectively. For the FS, there were significant differences in runoff rate under different rainfall intensities ( $P < 0.05$ ). Under weak rainfall intensity (0.6 mm/min), no runoff was recorded for the UFS. However, the FS produced a runoff under such conditions due to the existence of the frozen layer. The amount of slope erosion increased with the increase of rainfall intensity. Under the same treatments, the sediment yield rate was much higher in the II -stage than in the I -stage. When the rainfall intensity increased from 0.9 to 1.2 mm/min, the sediment yield rate of the FS and UFS increased 40.8% and 4.03% in the I -stage, respectively. And the sediment yield rates of the FS and UFS increased 93.8% and 36.81% in the II -stage, respectively. Besides, the amount of erosion on

the FS was much larger than that on the UFS. Under rainfall conditions of 0.9 and 1.2 mm/min, the sediment yield rate of the FS was 9.61 times and 7.10 times that of UFS in the I -stage, respectively. And the sediment yield rate of the FS was 6.1 times and 4.31 times that of UFS in the II -stage, respectively. For the FS, there was a significant difference in sediment yield under different rainfall intensity in the II -stage ( $P<0.05$ ). This demonstrated that the water was blocked via the frozen soil layer, which had a significant impact on hydraulic erosion.

### 3.1.2 Runoff and sediment yield under different treatments

Figure 3a shows the temporal variations in runoff rate under different rainfall intensities on the UFS and FS. The runoff rate under different treatments shows a typical pattern where the runoff intensity increased rapidly at the beginning of the rainfall before gradually stabilizing during the later period. The runoff rate of the FS quickly reached a steady state, while that of the UFS took a longer time to reach a stable state. Under the rainfall intensity of 0.9 mm/min, the runoff rate of FS became stable around the 15<sup>th</sup> min, while that of the UFS increased gradually until the 53<sup>rd</sup> min. For the rainfall intensity of 1.2 mm/min, the runoff rate for both slopes increased rapidly from 1<sup>st</sup> to 10<sup>th</sup> min after the start of the runoff, with the runoff rate of FS quickly approaching 1200 mm/min while that of the UFS reached 900 mm/min. Under the same rainfall intensity, the runoff yield rate was larger for the FS than for UFS (Fig. 3a), which indicated that the existence of the frozen layer reduces the initial runoff time of the slope on the one hand, and increased the flow intensity of the slope on the other hand, thus leading to an increase in the runoff yield rate of the slope. Further, the combined results of Table 1, Figures 2 and 3a suggested that the influence of rills on the slope runoff process was limited, since the slope runoff yield rate only changed slightly after the rills occurred.

Figure 3b presents the temporal variations in sediment yield rate under different rainfall intensity on the UFS and FS. Taking 1.2 mm/min as an example, for the FS, the process of sediment yield could be divided into two stages. The erosion in the I -stage (0–12 min) was dominated by inter-rill erosion, during which the sediment yield originates mainly from the erosion between the rills on the slope. The average sediment yield was only 139.65 g/min. During the II -stage, as small rill gradually appeared and the rapid development of rills occurred, the sediment yield rate increased to 523.00 g/min. The sediment yield on the UFS can also be characterized by two stages (Fig. 3b). During the I -stage (0–33 min), the inter-rill erosion dominates, and the sediment yield rate (19.67 g/min) was low, which represents only 14.09% of the FS. During the II -stage (33–60 min), rill erosion gradually appeared on the slope and the sediment yield rate increased drastically. The sediment yield rate at this stage was 121.46 g/min, which was only 0.23 times that of FS. These results demonstrated that the erosion process of the FS and UFS were similar, but the appearance of the rills on the FS occurred faster, developed more rapidly and led to a greater erosion intensity than on the UFS.

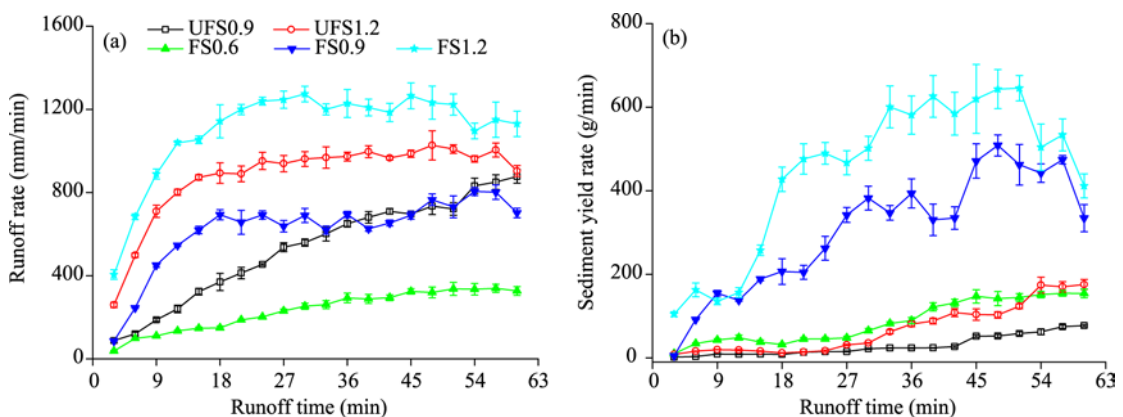


**Fig. 3** Temporal variations in runoff rate (a) and sediment yield rate (b) under different rainfall intensities. The numbers, 0.6, 0.9 and 1.2, after UFS and FS represent the rainfall intensities (mm/min).

### 3.1.3 Correlation between accumulative runoff and accumulative sediment yield

The process of soil erosion in this experiment was divided into the I -stage and II -stage. The former



is dominated by rainfall erosion, while the latter is dominated by runoff erosion. The entire slope erosion process obtained from our experiment was therefore analyzed according to these two stages. A function is fitted to the relationship between cumulative sediment yield and cumulative runoff of each field test. In the I -stage and II -stage, the cumulative sediment yield has a good fitting with the cumulative runoff as follows, respectively (Eqs. 3 and 4):

$$y = C_1x + D_1, \quad (3)$$

$$y = C_2x + D_2, \quad (4)$$

where  $y$  is the cumulative sediment yield (kg);  $x$  is the cumulative runoff (L); and  $C_1$ ,  $C_2$ ,  $D_1$  and  $D_2$  are regression coefficients (Table 2).

**Table 2** Cumulative runoff and cumulative sediment yield fitted equation under different erosion stages

Treatment	I –stage	MC <sub>1</sub>	II –stage	MC <sub>2</sub>
UFS0.9	$y = 0.033x - 3.052$ ( $R^2 = 0.9975^{**}$ )	0.027	$y = 0.049x - 37.537$ ( $R^2 = 0.9986^{**}$ )	0.066
UFS1.2	$y = 0.021x + 11.128$ ( $R^2 = 0.9823^{**}$ )		$y = 0.083x - 174.74$ ( $R^2 = 0.9786^{**}$ )	
FS0.6	$y = 0.269x + 23.462$ ( $R^2 = 0.9865^{**}$ )	0.247	$y = 0.424x - 142.10$ ( $R^2 = 0.9968^{**}$ )	0.487
FS0.9	$y = 0.297x - 3.618$ ( $R^2 = 0.9976^{**}$ )		$y = 0.575x - 469.78$ ( $R^2 = 0.9981^{**}$ )	
FS1.2	$y = 0.176x + 67.248$ ( $R^2 = 0.9861^{**}$ )		$y = 0.463x - 704.45$ ( $R^2 = 0.9972^{**}$ )	

Note: MC<sub>1</sub>, mean regression coefficient C<sub>1</sub>; MC<sub>2</sub>, mean regression coefficient C<sub>2</sub>; \*\*,  $P < 0.01$  level.

From the mathematical concept of the model and the actual runoff yield, the coefficients  $C_1$  and  $C_2$  are defined as the sediment yield coefficient. This coefficient was found to obey a certain change law. The  $C_1$  for the I -stage was always smaller than that for the II -stage. And the  $C_1$  and  $C_2$  of UFS were much smaller than those of FS. During the I -stage, the  $C_1$  of FS was 9 times (0.9 mm/min) and 8.38 times (1.2 mm/min) that of UFS, while during the II -stage, the  $C_2$  of FS was 11.73 times (0.9 mm/min) and 5.58 times (1.2 mm/min) that of the UFS.

### 3.2 Sorting characteristics of particles during the erosion process under different treatments

#### 3.2.1 Variation of MWD during slope erosion

While large differences exist between the variations of the MWD of eroded sediment particles on the UFS and FS, the time variations of MWD on the same type of slope under different rainfall intensities were consistent (Fig. 4a). Between 0 and 12 min after the beginning of the rainfall runoff, the MWD of particles on both slopes increased rapidly and became larger than that of the substrate particles. However, the MWD of particles on the FS was large and increased with the rainfall intensity while that of the UFS remained relatively small. Between 12 and 27 min, the MWD of both slopes decreased rapidly, with a sharper decrease for the FS. The MWD of both FS and UFS showed an increasing trend for 27–54 min, but with large fluctuations for the UFS particles, whereas the fluctuations for the FS were small. After the 54<sup>th</sup> minute, the MWD gradually stabilized for the both slopes and approached the substrate particle MWD. Under the conditions of this experiment, the change in MWD of the natural particles of eroded sediment is mainly influenced by the soil freeze–thaw and the slope runoff sorting characteristics. The average value of MWD was: UFS0.9 (73.84  $\mu\text{m}$ ) > FS0.6 (72.30  $\mu\text{m}$ ) > UFS1.2 (72.23  $\mu\text{m}$ ) > substrate (71.23  $\mu\text{m}$ ) > FS1.2 (71.06  $\mu\text{m}$ ) > FS0.9 (70.72  $\mu\text{m}$ ) (Fig. 4b). Under the same soil treatment, the MWD of eroded sediment particles did not differ significantly under different rainfall intensities ( $P > 0.05$ ). However, there were significant differences between UFS0.9 and FS0.9 and FS1.2 ( $P < 0.05$ ) in the MWD. Under the same rainfall intensity, the MWD of UFS was larger than that of the FS.

#### 3.2.2 Variation of different grain size sediment particles

The sediment sizes of the UFS and FS were classified as clay (<0.002 mm), fine silt (0.002–0.020 mm), coarse silt (0.020–0.050 mm) and fine sand (>0.050 mm). As shown in Figure 5, the clay contents were 0.200% for the loess. The clay (<0.002 mm) total content of the UFS and FS varied from 0.025% to 0.163%, suggested that little of the clay was dispersed. During the rainfall process, the percentage of the clay (<0.002 mm) remained stable for all treatments. The sediment was

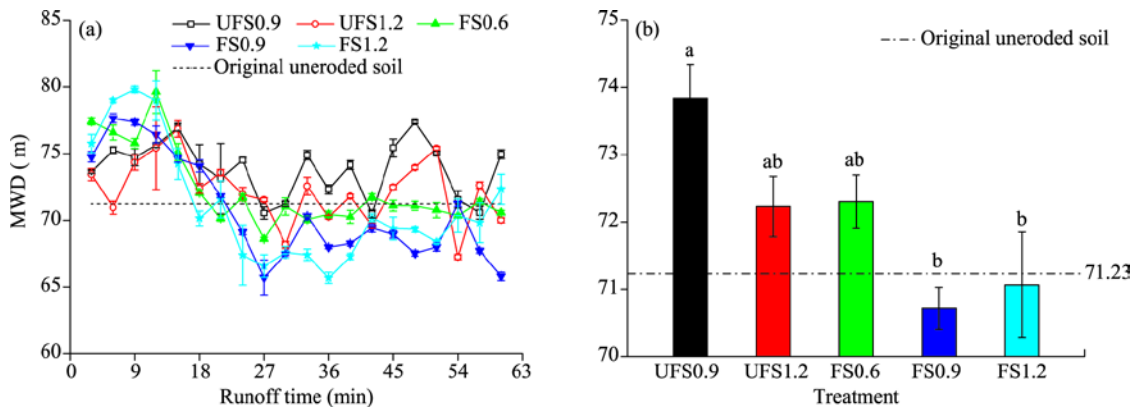


**Fig. 4** Temporal variations of the mean weight diameter (MWD) of particles (a) and the MWD (b). Different lowercase letters represent significant difference between different rainfall intensities at 0.05 level.

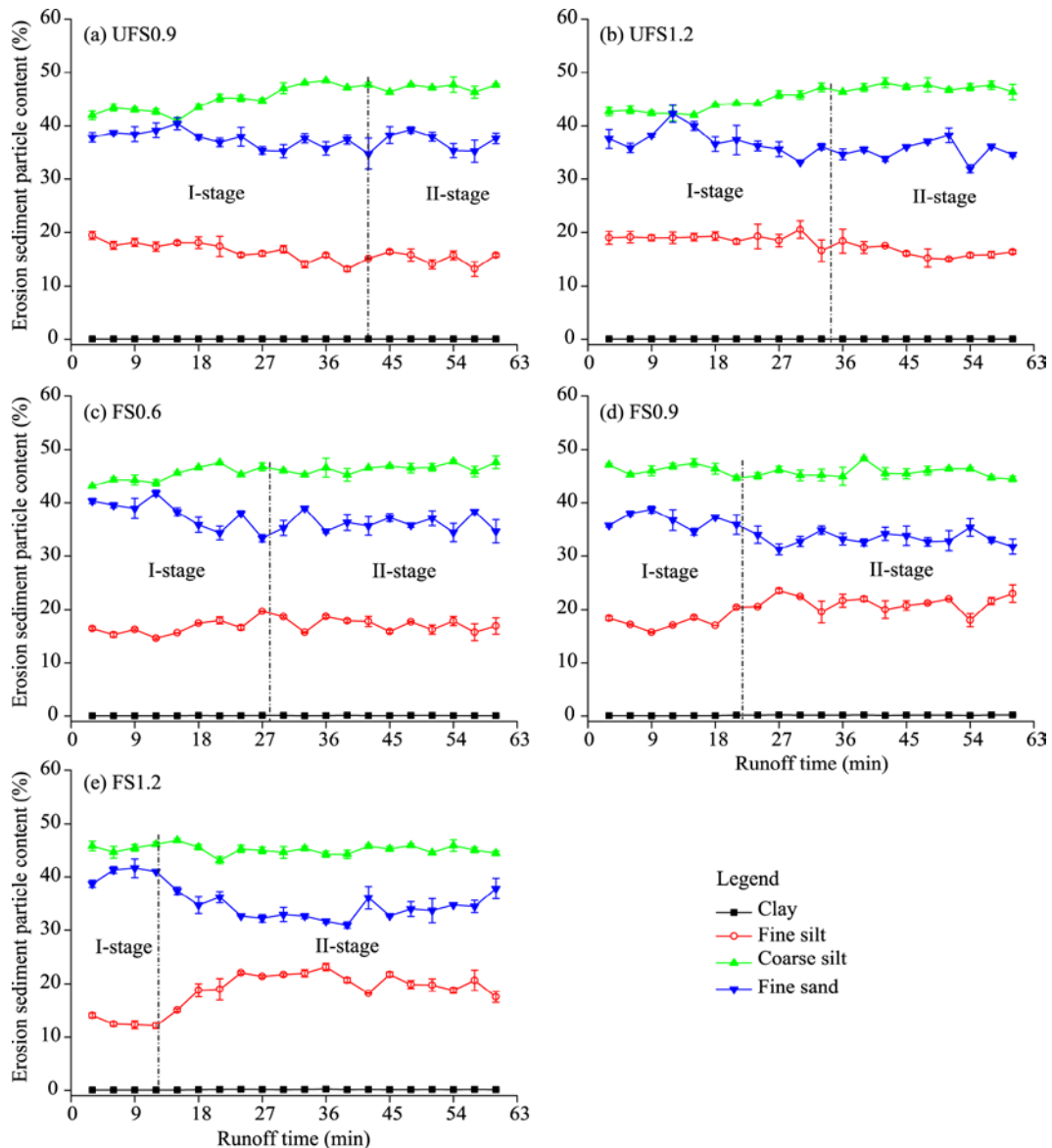


**Fig. 5** Temporal variations of eroded sediment particle contents under different soil treatments



principally composed of coarse silt (0.020–0.050 mm) and fine sand (>0.050 mm), which accounted for about 45% and 36% of the sediment, respectively (Table 3). Under different stages, the coarse silt content remained essentially unchanged with the rainfall intensity for the UFS and FS. The coarse silt content was greater for the FS than for UFS on the I -stage. The coarse silt and fine sand content of the FS were both smaller than those of the UFS on the II -stage. For the UFS, the fine silt content was greater on the I -stage than that on the II -stage. For the FS, the fine silt content was greater on the II -stage than that on the I -stage. Compared with the UFS, the FS had a larger content of fine silt.

**Table 3** Average percentage (%) of the effective particle size of sediment under different treatments

Treatment	Clay		Fine silt		Coarse silt		Fine sand	
	I-stage	II -stage	I-stage	II -stage	I-stage	II -stage	I-stage	II -stage
UFS0.9	0.030	0.025	16.753	15.162	44.733	47.237	37.615	36.945
UFS1.2	0.037	0.033	19.113	16.410	43.639	47.176	37.303	35.439
FS0.6	0.045	0.072	16.272	17.375	45.065	46.465	38.395	35.990
FS0.9	0.057	0.163	17.299	21.176	46.507	45.611	36.857	33.473
FS1.2	0.027	0.110	12.960	19.543	45.340	45.160	40.569	34.512

### 3.3 Soil erodibility

Estimates of soil erodibility based on measured data from the simulated rainfall tests (Table 4) demonstrate that the soil erodibility of FS is always greater than that of UFS under different rainfall intensities. The ratio of MK (mean soil erodibility) between the FS and UFS was 7.22 and the ratio of MC<sub>2</sub> between the FS and the UFS was 7.38. The two values were roughly the same. For the rainfall intensity of 0.9 and 1.2 mm/min, the soil erodibility of FS was 13.46 and 7.16 times that of the UFS, respectively. This result was consistent with the amount of slope erosion.

**Table 4** Soil erodibility factor (*K*) calculated from the rainfall simulation experiments for the UFS and FS

Treatment	<i>A</i> (kg/m <sup>2</sup> )	<i>MA</i> (kg/m <sup>2</sup> )	<i>R</i> (MJ·mm/(m <sup>2</sup> ·h))	<i>LS</i>	<i>K</i> (kg·h/(MJ·mm))	<i>MK</i> (kg·h/(MJ·mm))
UFS0.9	1.16	1.955	0.13	1.16	5.07	8.03
UFS1.2	2.75		0.14	1.16	10.99	
FS0.6	3.45	11.150	0.07	1.16	27.15	58.00
FS0.9	12.15		0.10	1.16	68.22	
FS1.2	17.85		0.13	1.16	78.64	

Note: *A*, amount of soil loss; *MA*, mean amount of soil loss; *R*, rainfall erosivity factor; *LS*, slope length and slope factor; *MK*, mean soil erodibility.

## 4 Discussion

### 4.1 Effects of freeze–thaw on slope erosion and sediment yield

As shown in Figure 3a, the FS had a higher runoff rate than UFS. The runoff rates of the FS and UFS were related to the thawing of the surface frozen layer. Li et al. (2009) confirms the significant effects of FS on runoff and infiltration. The FS produced a higher runoff volume compared with UFS during the experiments because the water present in the soil surface layer and the water in the soil pores condensed to form an "ice cap". At the beginning of the rainfall, the slope was still in a frozen state and the infiltration rate was small, so the flow rate was large. As the rainfall continued, the soil temperature on the slope increased, and the frozen soil within a certain depth from the surface gradually thawed, resulted in a similar runoff yield rate for the two slopes. These results were similar to those of previous studies (Øygarden, 2003; Zhou et al., 2009; Wang et al., 2018). As shown in Figure 3b, the FS had a larger sediment yield rate than UFS. During the rainfall process, the presence of a surface layer of frozen soil reduced infiltrations and increased the surface runoff and the erosion capacity. The increase in runoff in turn acts on the frozen soil, which prompted the thawed slope and continued to release erosive material (Zhang et al., 2018). The

feedback between the increased runoff and thawed accelerate the occurrence of erosion. During the test, a fluctuation in the amount of sediment yield occurred, which may be related to the development position and erosion mode of the rill. Numerous falling ridges were formed at the bottom of the slope, following which rills were formed, and the sediment yield increased. As the rainfall continued, the rills continued to develop, and the erosion was further aggravated, manifesting as traceability erosion and side wall collapse. By the end of the rainfall, the sediment yield increased significantly (Fig. 2), as a result of the inferior erosion and the large amount of slump (Wang, 2004). The linear-function relationships between the cumulative runoff and the sediment yield both under UFS and FS presented in this study lend a further support to the previously reported relationships (Wang et al., 2010; Xiao et al., 2011; Wang et al., 2017). The values of  $C_1$  and  $C_2$  may be related to the thawing rate of the slope, the depth of thawing and the degree of erosion development during rainfall.

#### **4.2 Effects of freeze–thaw on soil size selectivity**

The soil particles exhibited different size distribution during the process of erosion and transport, which reflected the changes affecting the erosion process (Fahrenhorst and Bryan, 1995; Sutherland et al., 1996). The dynamics of the runoff erosion of the UFS were limited, made it difficult to form longer rills (Fig. 2a). In the long period after the start of the runoff on the slope, soil erosion was dominated by inter-rill erosion, and the erosion particles are mainly fine particles; the fine silt content was higher, while the coarse silts content was relatively low. At the beginning of the runoff, the runoff rate of the FS increased rapidly, and the erosion power was large, resulted in higher content of coarse silts in the eroded sediment, while the content of fine silt was lower. As the rainfall continued, the gradual formation of rills occurred on the FS, and the slope gradually formed a slope-gully system (Fig. 2a). Following this, the erosive sediment was generated from the I -stage and II -stage. The I -stage usually caused fine particles to be enriched in sediment, while rill erosion had a weaker sorting effect on eroded sediment particles, resulted in a more complex composition of eroded sediment particles (Wan and El-Swaify, 1998). However, in the later period of rainfall, which saw the further development of rills, the amount of rill erosion accounts for a higher proportion of the total erosion, led to the gradual stabilization of the slope erosion particles, and a sediment particle distribution closed to the original one. During soil erosion, the difference in soil size selectivity between the UFS and FS may be due to the changes in soil properties caused by the soil frozen.

#### **4.3 Effects of freeze–thaw on soil erodibility**

Global climate change will cause the premature ablation of local frozen soil areas in seasonally freeze–thaw areas, thus changing the characteristics of hydraulic erosion. As differences in physical properties before and after soil frozen affect soil erodibility, the UFS and FS showed different erosion and sediment yield processes during the test (Wang et al., 2019, 2020). In this test, the erodibility of the soil after frozen was much greater than that of the control slope, which was consistent with the results of Wischmeier et al. (1971). When the soil freezes, the pore water between the soil particles generated various forms of ice crystal intrusion, resulting in an increase in soil volume. The expansion of ice crystals in the pores of the soil broke the bonds between the particles and changed the size of the agglomerates in the soil (Gatto, 2000). When the local temperature begins to rise, and the expansive soil began to melt and formed larger pores, the corrosion resistance of the soil decreased. The ratio of MK between the FS and UFS was 7.22. The ratio of  $MC_1$  and  $MC_2$  between the FS and UFS was 9.15 and 7.38, respectively. In the I -stage, the effect of freeze–thaw on soil erosion was large, and the sediment yield on FS was much larger than that on UFS. The ratio of MK between the FS and UFS was similar to the ratio of  $MC_2$ . This indicated that the soil erodibility can evaluate by the MK and  $MC_2$ . This finding was inconsistent with the results of Wang et al. (2017). However, it should be noted that the ratio of  $MC_2$  was not equal to the ratio of MK. The value of  $K$  only reflected the average condition of the soil. But the value of  $C_2$  may reflect changes in the accumulated sediments eroded under different soil treatments (UFS and FS) after the rills occurred. Therefore, the  $C_2$  could be an indicator for expressing the

soil erodibility in the II-stage. It can provide a reliable basis for predicting changes in local water erosion.

## 5 Conclusions

The initial runoff time of the FS was 6.4 to 18.7 min earlier than that of UFS under different rainfall intensities. The runoff and sediment yield of the FS were much larger than those of UFS; and the differences between the runoff and sediment yield on the FS and UFS were significant. However, it could be seen a similar pattern of rapid runoff increase followed by a stabilization in both cases. Under the same rainfall intensity, the occurrence of rills on the FS occurred 21 min earlier than that of UFS. The sediment yield of the UFS and FS can be divided into the I-stage and II-stage, but the FS had higher erosion intensity than the UFS. A linear relationship exists between the cumulative runoff and the cumulative sediment yield of the two slopes. The MWD on the slope erosion particles was as follows: UFS0.9 (73.84  $\mu\text{m}$ )>FS0.6 (72.30  $\mu\text{m}$ )>UFS1.2 (72.23  $\mu\text{m}$ )>substrate (71.23  $\mu\text{m}$ )>FS1.2 (71.06  $\mu\text{m}$ )>FS0.9 (70.72  $\mu\text{m}$ ). During the early stage of the rainfall, the MWD of FS was relatively large, with the coarse silt being preferentially transported. However, during the middle and late stage of rainfall, the transported particles on the FS gradually changed into fine silt and clay, and the particle composition gradually approached that of the soil substrate. The MK of FS is 7.22 times that of UFS. The ratio of the MC<sub>2</sub> between the FS and UFS was roughly correspondent with MK. Therefore, the C<sub>2</sub> could be used to evaluate soil erodibility after the appearance of the rills. This study improved our understanding of the effects of freeze–thaw and rainfall intensity on erosion processes. These results were only based on loess, so varying responses to more soil type by rainfall should be further investigated.

## Acknowledgements

This research was funded by the National Key Research and Development Program of China (2017YFC0403605), the National Natural Science Foundation of China (413517033), the State Key Laboratory of Simulation and Regulation of Water Cycle in River Basin, China Institute of Water Resources and Hydropower Research (SKL2018CG04), and the Shaanxi Province Innovation Talent Promotion Plan Project Technology Innovation Team (2018TD-037). We thank the reviewers for their useful comments and suggestions.

## References

- Asadi H, Ghadiri H, Rose C W, et al. 2007. An investigation of flow-driven soil erosion processes at low streampowers. *Journal of Hydrology*, 342(1–2): 134–142.
- Bissonnais Y L. 1996. Aggregate stability and assessment of soil crustability and erodibility: I. Theory and methodology. *European Journal of Soil Science*, 47(4): 425–437.
- Bochove E V, Danielle P, Pelletier F. 2000. Effects of freeze–thaw and soil structure on nitrous oxide produced in a clay soil. *Soil Science Society of America Journal*, 64(5): 1638–1643.
- Bullock M S, Nelson S D, Kemper W D. 1988. Soil cohesion as affected by freezing, water content, time and tillage. *Soil Science Society of America Journal*, 52(3): 770–776.
- Chang E H, Li P, Li Z B, et al. 2019a. Using water isotopes to analyze water uptake during vegetation succession on abandoned cropland on the Loess Plateau, China. *Catena*, 181: 104095.
- Chang E H, Li P, Li Z B, et al. 2019b. The impact of vegetation successional status on slope runoff erosion in the Loess Plateau of China. *Water*, 11(12): 2614.
- Cheng Y T, Li P, Xu G C. 2018. The effect of soil water content and erodibility on losses of available nitrogen and phosphorus in simulated freeze–thaw conditions. *Catena*, 166: 21–33.
- Cruse R M, Mier R, Mize C W. 2001. Surface residue effects on erosion of thawing soils. *Soil Science Society of America Journal*, 65(1): 178–184.
- Dagesse D F. 2010. Freezing-induced bulk soil volume changes. *Canadian Journal of Soil Science*, 90(3): 389–401.
- Edwards L M, Burney J R. 1989. The effect of antecedent freeze–thaw frequency on runoff and soil loss from frozen soil with and without subsoil compaction and ground cover. *Canadian Journal of Soil Science*, 69(4): 799–811.
- Farenhorst A, Bryan R B. 1995. Particle size distribution of sediment transported by shallow flow. *Catena*, 25(1–4): 47–62.

- Ferrick M G, Gatto L W. 2005. Quantifying the effect of a freeze–thaw cycle on soil erosion: laboratory experiments. *Earth Surface Processes and Landforms*, 30(10): 1305–1326.
- Gatto L W. 2000. Soil freeze–thaw–induced changes to a simulated rill: potential impacts on soil erosion. *Geomorphology*, 32(1): 147–160.
- Henry H A L. 2007. Soil freeze–thaw cycle experiments: Trends, methodological weaknesses and suggested improvements. *Soil Biology and Biochemistry*, 39(5): 977–986.
- Issa O M, Bissonnais Y L, Planchon O. 2006. Soil detachment and transport on field- and laboratory-scale interrill areas: Erosion processes and the size-selectivity of eroded sediment. *Earth Surface Processes and Landforms*, 31(8): 929–939.
- Kirkby M J. 1980. Modelling water erosion processes. In: Kirkby M J, Morgan R P C. *Soil Erosion*. Chichester: Wiley, 183–196.
- Koiter A J, Owens P N, Petticrew E L. 2013. The behavioural characteristics of sediment properties and their implications for sediment fingerprinting as an approach for identifying sediment sources in river basins. *Earth-Science Reviews*, 125: 24–42.
- Layton J B, Skidmore E L, Thompson C A. 1993. Winter-associated changes in dry-soil aggregation as influenced by management. *Soil Science Society of America Journal*, 57(6): 1568.
- Li G Y, Fan H M. 2014. Effect of freeze–thaw on water stability of aggregates in a black soil of northeast China. *Pedosphere*, 24(2): 285–290.
- Li X, Jin R, Pan X D. 2012. Changes in the near-surface soil freeze–thaw cycle on the Qinghai-Tibetan Plateau. *International Journal of Applied Earth Observation and Geoinformation*, 17: 33–42.
- Li Z, Wu P T, Feng H, et al. 2009. Simulated experiment on effect of soil bulk density on soil infiltration capacity. *Transactions of the CSAE*, 25(6): 40–44. (in Chinese)
- Øygarden L. 2003. Rill and gully development during an extreme winter runoff event in Norway. *Catena*, 50(2–4): 217–242.
- Oztas T, Fayetorbay F. 2003. Effect of freezing and thawing processes on soil aggregate stability. *Catena*, 52(1): 1–8.
- Pawluk S. 1988. Freeze–thaw effects on granular structure reorganization for soil materials of varying texture and moisture content. *Canadian Journal of Soil Science*, 68(3): 485–494.
- Ren Z P, Su Y Y, Li P, et al. 2018. Runoff scouring experiment on sand-covered slope. *Journal of Soil and Water Conservation*, 32(3): 29–35, 41. (in Chinese)
- Sahin U, Anapali O. 2007. Short communication: The effect of freeze–thaw cycles on soil aggregate stability in different salinity and sodicity conditions. *Spanish Journal of Agricultural Research*, 5(3): 431–434.
- Sharratt B S, Lindstrom M J, Benoit G R, et al. 2000. Runoff and soil erosion during spring thaw in the Northern U.S. Corn Belt. *Journal of Soil and Water Conservation*, 55(4): 487–494.
- Shen H O, Zheng F L, Wen L L, et al. 2016. Impacts of rainfall intensity and slope gradient on rill erosion processes at loessial hillslope. *Soil and Tillage Research*, 155: 429–436.
- Shi P, Qin Y, Liu Q, et al. 2019. Soil respiration and response of carbon source changes to vegetation restoration in the Loess Plateau, China. *Science of the Total Environment*, 707: 135507, doi: 10.1016/j.scitotenv.2019.135507.
- Shi P, Feng Z H, Gao H D, et al. 2020. Has "Grain for Green" threaten food security on the Loess Plateau of China? *Ecosystem Health and Sustainability*, 6(1): 1709560, doi: 10.1080/20964129.2019.1709560.
- Shi Z H, Fang N F, Wu F Z, et al. 2012. Soil erosion processes and sediment sorting associated with transport mechanisms on steep slopes. *Journal of Hydrology*, 454–455: 123–130.
- Su Y Y, Li P, Ren Z P, et al. 2020. Slope erosion and hydraulics during thawing of the sand-covered Loess Plateau. *Water*, 12(9): 2461.
- Sutherland R A, Wan Y, Ziegler A D, et al. 1996. Splash and wash dynamics: an experimental investigation using an oxisol. *Geoderma*, 69(1): 85–103.
- Ting J M, Torrence, Martin R, et al. 1983. Mechanisms of strength for frozen sand. *Journal of Geotechnical Engineering*, 109(10): 1286–1302.
- Wan Y, El-Swaify S A. 1998. Characterizing interrill sediment size by partitioning splash and wash processes. *Soil Science Society of America Journal*, 62(2): 430.
- Wang B, Zheng F, Römken M J M. 2013. Soil erodibility for water erosion: A perspective and Chinese experiences. *Geomorphology*, 187(1): 1–10.
- Wang L, Tang L L, Wang X, et al. 2010. Effects of alley crop planting on soil and nutrient losses in the citrus orchards of the three gorges region. *Soil and Tillage Research*, 110(2): 243–250.
- Wang L, Shi Z H, Wang J. 2014. Rainfall kinetic energy controlling erosion processes and sediment sorting on steep hillslopes: A case study of clay loam soil from the Loess Plateau, China. *Journal of Hydrology*, 512: 168–176.
- Wang L, Wang Y, Saskia K, et al. 2018. Effect of soil management on soil erosion on sloping farmland during crop growth stages under a large-scale rainfall simulation experiment, 10(6): 921–931.

- Wang S J. 2004. Characteristics of freeze and thaw weathering and its contribution to sediment yield in middle yellow river basin. *Bulletin of Soil and Water Conservation*, 24(6): 1–5. (in Chinese)
- Wang T, Li P, Ren Z P, et al. 2017. Effects of freeze–thaw on soil erosion processes and sediment selectivity under simulated rainfall. *Journal of Arid Land*, 9(2): 234–243.
- Wang T, Li P, Hou J M, et al. 2018. Response of the meltwater erosion to runoff energy consumption on loessal slopes. *Water*, 10(11): 1522.
- Wang T, Li P, Li Z B, et al. 2019. The effects of freeze–thaw process on soil water migration in dam and slope farmland on the Loess Plateau, China. *Science of The Total Environment*, 666: 721–730.
- Wang T, Li P, Liu Y, et al. 2020. Experimental investigation of freeze–thaw meltwater compound erosion and runoff energy consumption on loessal slopes. *Catena*, 185: 104310.
- Wang W B, Shu X, Zhang Q F. 2015. Effects of freeze–thaw cycles on the soil nutrient balances, infiltration, and stability of cyanobacterial soil crusts in northern China. *Plant and Soil*, 386(1–2): 263–272.
- Weindorf D C. 2006. Relationships between permeability and erodibility of cultivated acrisols and cambisols in subtropical China. *Pedosphere*, 16(3): 34–41.
- Wischmeier W H, Smith D D. 1965. Predicting rainfall erosion losses: a guide to conservation planning. *Agriculture Handbook*. Washington D C, United States Department of Agriculture, 537: 5–8.
- Wischmeier W H, Johnson C B, Cross B V. 1971. A soil erodibility nomograph for farmland and construction sites. *Journal of Soil Water Conservation*, 26: 93–189.
- Xiao L, Yao K H, Li P, et al. 2019a. Effects of freeze–thaw cycles and initial soil moisture content on soil aggregate stability in natural grassland and Chinese pine forest on the Loess Plateau of China. *Journal of Soils and Sediments*, 20(3): 1222–1230.
- Xiao L, Zhang Y, Li P, et al. 2019b. Effects of freeze–thaw cycles on aggregate–associated organic carbon and glomalin-related soil protein in natural-succession grassland and Chinese pine forest on the Loess Plateau. *Geoderma*, 334: 1–8.
- Xiao P Q, Yao W Y, Shen Z Z, et al. 2011. Experimental study on erosion process and hydrodynamics mechanism of alfalfa grassland. *Journal of Hydraulic Engineering*, 42(2): 232–237. (in Chinese)
- Zhang Y, Zhang H, Li Z B. 2018. Process of runoff and sediment yield and relationship between water and sand of frozen soil slope in loess area under different rainfall intensities. *Transactions of the Chinese Society of Agricultural Engineering*, 34(11): 136–14. (in Chinese)
- Zhang Y, Li P, Liu X J, et al. 2019. Effects of farmland conversion on the stoichiometry of carbon, nitrogen, and phosphorus in soil aggregates on the Loess Plateau of China. *Geoderma*, 351: 188–196.
- Zhao B H, Li Z B, Li P, et al. 2017. Spatial distribution of soil organic carbon and its influencing factors under the condition of ecological construction in a hilly-gully watershed of the Loess Plateau, China. *Geoderma*, 296: 10–17.
- Zhou L L, Wang T L, Fan H M. 2009. Effects of incompletely thawed layer on black soil slope rainfall erosion. *Journal of Soil and Water Conservation*, 23(6): 1–4, 37. (in Chinese)